RSC Advances

ROYAL SOCIETY OF CHEMISTRY

www.rsc.org/advances

A New 3D Framework Based on Reduced Wells-Dawson Arsenotungstates as Eight-connected Linkages†

Wenlong Sun, Shaobin Li, Huiyuan Ma*, Haijun Pang*, Li Zhang and Zhuanfang Zhang

Key Laboratory of Green Chemical Engineering and Technology of College of Heilongjiang Province, College of Chemical and Environmental Engineering, Harbin University of Science and Technology, Harbin 150040, China Tel.: 86-0451-86392716, Fax: 86-0451-86392716; E-mail: mahy017@163.com (Ma H. Y.), panghj116@163.com (Pang. H. J.).

†Electronic supplementary information (ESI) available: CIF file of **1**; Additional figures . See DOI:

A new hybrid compound based on reduced Wells-Dawson arsenotungstates as eight-connected linkages, $[Cu_4(btb)_6(H_2O)_2][As_2W^{V}_2W^{VI}_{16}O_{62}]\cdot 10H_2O$ (**1**) (btb = 1,4-bis(1,2,4-triazol-1-y1)butane) has been synthesized under hydrothermal conditions. Structural analysis shows that **1** displays a 3D POMOF structure consisting of two crystal distinct motifs: 3D MOF architecture and eight-connected As_2W_{18} cluster. It is worth mentioning that the 3D MOF architecture possesses two kinds of channels (A and B). The eight-connected As_2W_{18} clusters as guests occupy the B channels and incorporate with the MOF to achieve 3D POMOF architecture with a novel $(3^2\cdot4^2\cdot5^2)(3^3\cdot4^5\cdot5^3\cdot6^4)_2(3^6\cdot4^9\cdot5^9\cdot6^4)$ topology. In addition, the electrochemical studies show that **1** has good electrocatalytic activities toward reduction of both hydrogen peroxide and nitrite molecules ascribed to W-centers. The photocatalytic properties of **1** indicate that the title compound presents a good degradation activity and may be a potential photocatalyst to oxidative the

decomposition of Methylene Blue dye.

Introduction

Polyoxometalates (POMs), as a large family of metal-oxygen clusters, have been extensively studied due to their enormous structural variety and intriguing properties in chemistry, physics, catalysis, and materials science.[1-10] They cover an enormous range in size and structure and thereby provide an access to a huge library of readily available and controllable second building units (SBUs). The POMs as SBUs can link variable transition-metal complexes (TMCs) for construction of various multifunctional hybrid materials with combination of key merits of both components.[11-14] Among the reported hybrid materials, those compounds with both high-connectivity and high-dimensionality structures have drawn more and more attention of chemists, because generally there exists a correlation between their complexity of structures and functionalities predicted early by Zubieta.[15] To construct high-connected and high-dimensional POM based hybrid compounds, one effective method is to increase the surface charge density of POM polyanions. The higher charge density will lead to a higher affinity to interact with TMCs, which possibly results in forming the high-connected structures with ease. Generally, there are mainly two strategies widely adopted for increasing the surface charge density of POMs: (I) the transition metal substituted POMs (replacing high-oxidation state metals of POMs with other lower-valence metals) and (II) the heteropoly blue POMs (reducing the metal centers of POMs). To date, thanks to the work of POM chemists, some novel high-connected and high-dimensional hybrid compounds have been successfully

synthesized with strategy I.[16-18] Nevertheless, the high-connected and high-dimensional hybrid compounds constructed by strategy II are rarely obtained,[19] though such materials are of considerable significance in magnetochemistry and materials science.[20]

In our previous work, a new 3D hybrid compound with dimeric monocopper-substituted Keggin polyoxoanions as ten-connected linkages, $[Cu_5(en)_9][(PW_{11}CuO_{39})_2]\cdot 18H_2O$ (en = ethylenediamine), has been synthesized *via* the strategy I.[21] In our present, we try to obtain high-connected and high-dimensional hybrid compounds by strategy II. With this aim in mind, the reduced Wells-Dawson polyanion captures our attention since they possess more surface oxygen atoms (18 terminal O atoms and 36 μ_2-O atoms) than other well-known POMs, such as Keggin, Anderson, and Lindqvist. The surface oxygen atoms with high electron density in the reduced Wells-Dawson polyanion as the potential coordination sites can effectively connect with the TMCs. To our knowledge, the high-connected and high-dimensional hybrids based on Wells-Dawson arsenotungstates are rarely reported,[22] and the highest number of the connecting sites of Wells-Dawson arsenotungstate anions is limited to seven. In addition, another important factor of the rational design of hybrids is judicious choice of organic ligands. Among many multidentate N-donor ligands, flexible 1,4-bis (1,2,4-triazol-1-y1)butane (abbr btb) molecule is a good candidate for construction high-connected and high-dimensional hybrids. Because the 1, 2, 4-triazole group of btb ligand, with three N donors, is an integration of the coordination geometry of both imidazoles and pyrazoles to provide more potential

coordination sites **(Scheme S1)**, and this kind of ligand exhibits a strong and typical coordination capacity to construct the metal-organic frameworks (MOFs) with high-dimension.[23]

Herein, we report the preparation and structure of a new 3D hybrid compound based on reduced Wells-Dawson arsenotungstates, $[Cu_4(btb)_6(H_2O)_2][As_2W^V_2W^{VI}_{16}O_{62}]\cdot 10H_2O$ (**1**), which exhibits a 8-connected 3D framework with a novel $(3^2\cdot4^2\cdot5^2)(3^3\cdot4^5\cdot5^3\cdot6^4)_2(3^6\cdot4^9\cdot5^9\cdot6^4)$ topology. To the best of our knowledge, it represents the first hybrid compound based on the reduced-polyanion $[As_2W^V_2W^{VI}_{16}O_{62}]^{8-}$ with a high connectivity and dimensionality structure to date. In addition, the electrocatalytic and photocatalytic properties of **1** were also investigated in details.

Experimental Section

Materials and general methods

The α-$K_6As_2W_{18}O_{62}\cdot 14H_2O$ was prepared according to the literature method.[24] All other chemicals were commercially purchased and used without purification. Elemental analyses (C, H and N) were performed on a Perkin-Elmer 2400 CHN Elemental Analyzer, and that of As, Cu and W were carried out with a Leaman inductively coupled plasma (ICP) spectrometer. The FT-IR spectrum was recorded from KBr pellets in the range 4000–400 cm^{-1} with a Nicolet AVATAR FT-IR360 spectrometer. A CHI660 electrochemical workstation was used for control of the electrochemical measurements and data collection. A conventional three-electrode system was used, with carbon paste electrode (CPE) as working electrode,

commercial Ag/AgCl as reference electrode and twisted platinum wire as counter electrode. The powder X-ray diffraction (PXRD) data were collected on Rigaku RINT2000 diffractometer at room temperature. UV-vis absorption spectra were recorded on a 756 CRT UV-vis spectrophotometer.

Synthesis of $[Cu_4(btb)_6(H_2O)_2][As_2W^{V}_2W^{VI}_{16}O_{62}]\cdot 10H_2O$ (1)

A mixture of α-$K_6As_2W_{18}O_{62}\cdot 14H_2O$ (0.35 g, 0.073 mmol), $Cu(NO_3)_2\cdot 3H_2O$ (0.15 g, 0.6 mmol), btb (0.085 g, 0.44 mmol) and Et_3N (0.2 mL) was dissolved in 20 mL of distilled water at room temperature. Then the pH value of the mixture was adjusted to about 3.8 with 1.0 mol L^{-1} NaOH, and the obtained suspension was put into Teflon-lined autoclave and kept under autogenous pressure at 170 °C for 4 days. After slow cooling to room temperature, green rhombic block crystals of **1** were filtered, washed with distilled water and dried at room temperature. Yield: 51 % (based on W). Anal. calcd. for **1**: H, 1.59; C, 9.49; N, 8.30; Cu, 4.18; As, 2.47; W, 54.48 (%). Found: H, 1.51; C, 9.59; N, 8.37; Cu, 4.04; As, 2.56; W, 54.61 (%).

X-ray Crystallography

Single-crystal X-ray diffraction data collection of **1** was performed using a Bruker Smart Apex CCD diffractometer with Mo-*Ka* radiation (λ = 0.71073 Å) at 293 K. Absorption corrections were applied by using the multiscan program SADABS.[25] The structures were solved by direct methods, and non-hydrogen atoms were refined anisotropically by least-squares on F^2 using the SHELXTL program.[26] The hydrogen atoms of organic ligands were generated geometrically for **1**, while the hydrogen atoms of water molecules can not be found from the residual peaks and were directly

included in the final molecular formula. The reported refinement of **1** is of the guest-free structures using the *.hkp file produced by using the *SQUEEZE* routine. There are at least ten solvent water molecules in the crystal structure of **1**. These water molecules were directly included in the final molecular formula based on the elemental analysis, TG and SQUEEZE analyses. A summary of the crystal data, data collection, and refinement parameters for **1** are listed in Table 1. Crystallographic data for the structures reported in this paper have been deposited in the Cambridge Crystallographic Data Center with CCDC Number: 989568.

Table 1 Crystal data and structure refinements for **1**.

Compound	**1**
Formula	$C_{48}H_{96}As_2Cu_4N_{36}O_{74}W_{18}$
Formula weight	6074.58
Crystal system	Monoclinic
Space group	*C2/c*
a/Å	16.207(5)
b/Å	25.341(5)
c/Å	29.606(5)
β/°	92.522(5)
V/Å^3	12148(5)
Z	4
D_{calcd}/g cm^{-3}	3.221
T/K	293(2)
μ/mm^{-1}	18.286
Refl. Measured	30559
Refl. Unique	10701
R_{int}	0.0730
GoF on F^2	0.901
R_1/wR_2 [$I \geq 2\sigma(I)$]	0.0590/0.1639

$R_1 = \sum \| F_o | - | F_c \| / \sum | F_o |$. $wR_2 = \sum[w(F_o^2 - F_c^2)^2] / \sum[w(F_o^2)^2]^{1/2}$

Results and discussion

Description of crystal structure

The single-crystal X-ray diffraction analysis study reveals that **1** crystallizes in the

monoclinic space group *C2/c* (No. 15). The asymmetric unit of **1** includes one $[As_2W^{V}_2W^{VI}_{16}O_{62}]^{8-}$ (abbreviated to As_2W_{18}) polyanion, four Cu cations, six btb ligands and two coordinated water molecules (Fig. 1a). The reduced-polyanion As_2W_{18} shows a classical Wells-Dawson structure, and possesses higher charge density than common saturated Wells-Dawson polyanion, which makes them favorable for formation of complicated structures. As shown in Fig. 1b, each As_2W_{18} cluster acts as octadentate inorganic ligand covalently bonding to eight Cu ions (Cu1, Cu2, Cu3, $Cu1^{\#1}$, $Cu1^{\#2}$, $Cu1^{\#3}$, $Cu2^{\#1}$ and $Cu3^{\#1}$), which represents its highest connected number to date. There are three crystallographically independent Cu ions in **1**, which shows similar distorted octahedral coordination geometry but different coordination environments (Fig. S1). The coordination environments of Cu1 and Cu2 are identical, which are coordinated by two oxygen atoms from two As_2W_{18} anions and four nitrogen atoms from four btb ligands. The Cu3 is coordinated by four oxygen atoms from two water molecules and two As_2W_{18} anions as well as two nitrogen atoms from two btb ligands. The bond lengths and angles around the Cu ions are in the ranges of 1.96(3)−2.10(2) Å (Cu−N), 1.97(2)−2.39(2) Å (Cu−O), 81.0(10)−180.0(9)° (N−Cu−N) and 87.5(4)−92.5(4)° (N−Cu−O). All of these bond lengths and angles are within the normal ranges observed in other Cu(II)-containing complexes.[27]

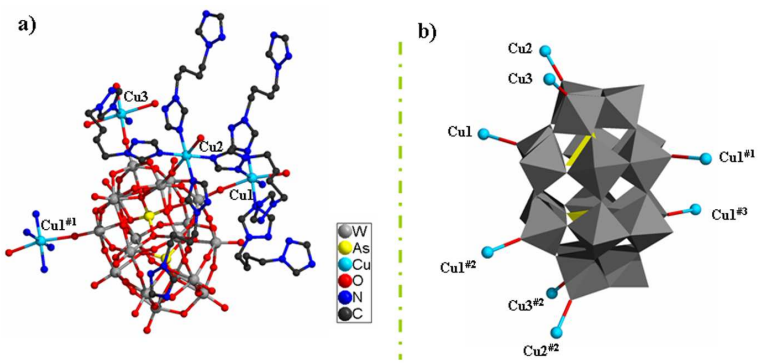

Fig. 1. View of (a) the basic crystallographic unit in **1** and (b) the polyhedral/ball representation of the coordination mode of As_2W_{18} cluster (Symmetry code: #1, x, -1+y, z; #2, 1-x, -y, 2-z; #3, 2-x, 1+y, 1-z.).

One of the structural features of **1** is that 2D undulated layer with 48-membered macrocycle (Fig. S3) was constructed by left-, right-handed helixes, and a meso-helix (Fig. 2 and Fig. 3a). There are four crystallography independent btb (btb1, btb2, btb3 and btb4) ligands in **1** and they show two types of conformation modes: "U"-type and "Z"-type. Meanwhile, there are two kinds of coordinated modes (μ_2 and μ_3) for btb ligands in **1**: the 1, 2, 4-triazole group of imidazoles potential coordination N donors in btb ligands are utilized to coordinate with two or three Cu cations, respectively (Fig. S2). Both the btb1 and btb2 ligands adopting the same μ_2 mode link Cu1 cations to form left- and right-handed helixes, and the btb4 ligands adopting μ_3 mode link Cu2 and Cu3 cations to form an extraordinary meso-helix. In fact, to the best of our knowledge, only two POM-based helical compounds possessing both common helix and meso-helix in one compound have been reported up to now.[28] Therefore, **1** represents a new example of such compound that is coexistence of common helix and meso-helix.

Another structural feature of **1** is its intricate 3D POMOF architecture that can be described in the as follows: the btb3 ligands by μ_2 mode link these parallel 2D

undulated layers forming a 3D MOF architecture with two kinds of channels (A and B). Finally, the eight-connected As_2W_{18} clusters as guests occupy the B channels and incorporate with the MOF to achieve 3D POMOF architecture (Fig. 3c). From the topological view, if Cu1 and Cu2 cations are considered as 6-connected nodes and the Cu3 cations as well as As_2W_{18} clusters are considered as 4- and 8-connected nodes, respectively. The structure of **1** can be simplified as a novel 3D (4, 6, 6, 8)-connected framework with a $(3^2\cdot4^2\cdot5^2)(3^3\cdot4^5\cdot5^3\cdot6^4)_2(3^6\cdot4^9\cdot5^9\cdot6^4)$ topology (Fig. 3d).

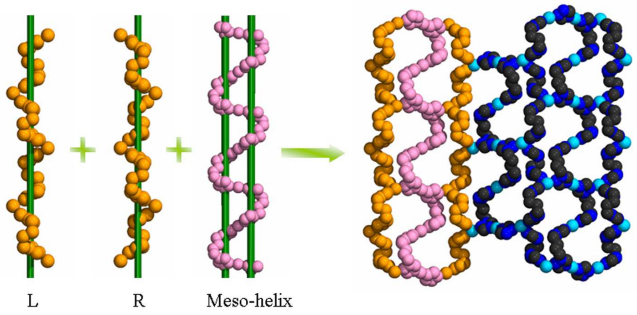

Fig. 2. A 2D layer connected by the left-handed, right-handed helical and Meso-helical chains.

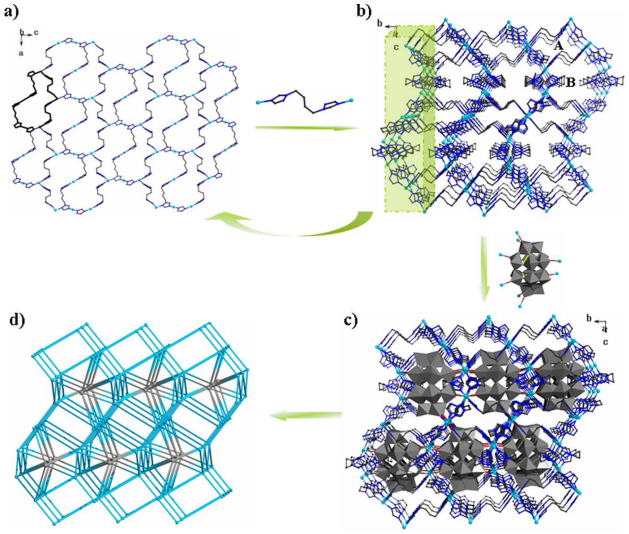

Fig. 3. View of (a) the 2D undulated layer with 48-membered macrocycle, (b) the 3D MOF in **1**, (c) the 3D POMOF structure and (d) Schematic view of the $(3^2\cdot4^2\cdot5^2)(3^3\cdot4^5\cdot5^3\cdot6^4)_2(3^6\cdot4^9\cdot5^9\cdot6^4)$ topology in **1**. Colour codes: blue, the Cu cations; gray, the As_2W_{18} anions.

Analyses of BVS, XPS, IR, XRPD and TG measurements

Compound **1** was synthesized under hydrothermal conditions. All copper atoms in **1**

are in the +II oxidation state, confirmed by their octahedral coordination environments, blue crystal color and BVS calculations.[29] The XPS spectrum of **1** shows two overlapped peaks at 35.12 eV and 37.21 eV (Fig. S4), which are attributed to W^{V} and W^{VI}, respectively.[30] All of these results consist with the structural analyses and charge balance. In the synthetic process of **1**, the W(VI) was partly reduced to W(V). The triethylamine in this reaction may be acted as not only mineralization agent but also reducing agent. Such phenomena have often been observed in reactions of organic amine under hydrothermal conditions.[19e, 31]

As shown in Fig. S5, the IR spectrum exhibits the characteristic peaks at 1069, 961, 869 and 784 cm^{-1} in **1**, which are attributed to ν(As-O), ν(W=Ot), ν_{as}(W–Ob–W) and ν_{as}(W–Oc–W), respectively. Compared to the typical Wells-Dawson type heteropolyanion As_2W_{18}, compound **1** has similar peaks in the range of 780–1080 cm^{-1} except for slight shifts of peaks due to the interactions between the polyanions and the Cu^{2+} cations in the solid state, which indicates that the As_2W_{18} cluster in title compound still retains the basic structure of Wells-Dawson As_2W_{18} polyanion.[32] Additionally, the characteristic peaks in the region 1621 to 1268 cm^{-1} could be ascribed to the character peaks of btb ligands.[23a]

The PXRD patterns for **1** are presented in the Fig. S6. The diffraction peaks of both simulated and experimental patterns match well, thus indicating that the phase purities of the **1** are good. The difference in reflection intensities between the simulated and the experimental patterns is due to the different orientation of the crystals in the powder samples.

The TG curve of **1** (Fig. S7) shows two-step weight loss in the temperature range of 30 to 600 ºC. The first weight loss of 4.27 % (Calc. 4.15 %) in the temperature range of 30 to 250 ºC, corresponding to the loss of water molecules. The second weight loss of 22.58 % (Calc. 20.32 %) in the temperature range of 250 to 600 ºC is observed corresponding to the decomposition of organic btb molecules and collapse of As_2W_{18} cluster. The whole weight loss of 26.85 % is in agreement with the calculated value 24.47 %.

Electrochemical properties

The POMs possess the ability of undergoing reversible multi-electron redox processes, which makes them very attractive in chemically-modified electrode and the electrocatalytic study.[33] Due to the title compounds are insoluble in water and common organic solvents. Thus, the bulk-modified carbon paste electrode (CPE) becomes the optimal choice to study the electrochemical properties, which is inexpensive, easy to prepare and handle.[34]

The cyclic voltammetric behavior for **1**-CPE (carbon paste electrode) was studied in 1 M H_2SO_4 solution (Fig. 4). In the potential range of -0.7 to 0.4 V, there exist three redox peaks with half-wave potentials E1/2 at -0.08 (II-II'), -0.28 (III-III') and -0.54 V (IV-IV'), which can be ascribed to redox processes of tungstate in **1**. In addition, there is one irreversible anodic peak (I) at +0.2 V, which is assigned to the oxidation of copper.[35] As shown in the insert of Fig. 4, when the scan rates are varied from 0.1 to 0.6 $V \cdot s^{-1}$, the peak potentials change gradually: the cathodic peak potentials shift toward the negative direction and the corresponding anodic peak

potentials to the positive direction with increasing scan rates. The peak currents are proportional to the scan rate, which indicate that the redox processes are surface-controlled.[36]

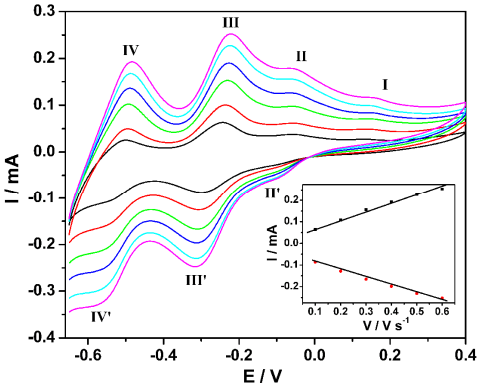

Fig. 4. Cyclic voltammograms for **1**-CPE in 1 M H_2SO_4 solution at different scan rates (from inner to outer): 0.1, 0.2, 0.3, 0.4, 0.5, 0.6 V s^{-1}.The inset shows plots of the anodic and the cathodic peak currents for III againt scan rates.

The POMs have been exploited extensively in electrocatalytic reactions and further applications such as biosensors and fuel cells.[37] Herein, the reduction of hydrogen peroxide (H_2O_2) and nitrite (NO_2^-) were chosen as test reaction to study the electrocatalytic activity of **1**. As shown in Fig. 5, it displays good electrocatalytic activity toward the reduction of H_2O_2 and NO_2^- in 1 M H_2SO_4 solution. With the addition of H_2O_2 and NO_2^-, the cathodic peak IV substantially increased, while the corresponding anodic peak currents decreased. The inset of Fig. 5 a and b show the relationship between the fourth cathodic current and concentration of H_2O_2 and NO_2^-. The electrocatalytic efficiency of **1**-CPE (based on a rough calculation using CAT formula)[38] toward the reduction of H_2O_2 and NO_2^- were *ca.* 95% and 120% at 1M H_2SO_4 containing 50 mM hydrogen peroxide and nitrite, which suggests that **1** has potential applications in detection of hydrogen peroxide and nitrite.

The performance of the parent POM clusters ($(NBu_4)_6[As_2W_{18}O_{62}]$) and compound **1** has been compared. As shown in Fig. S8, it can be seen that the parent POM cluster $(NBu_4)_6[As_2W_{18}O_{62}]$ almost have no electrocatalytic reduction activities towards hydrogen peroxide (H_2O_2) and nitrite (NO_2^-). However, the electrochemical studies showed that compound **1** have good electrocatalytic activity toward the reduction of H_2O_2 and NO_2^-, thanks to the complicated 3D structure of compound **1** that enhances the electrocatalytic reduction activities. Additionally, the stability experiment for **1**-CPE has been investigated scanning for 40 cycles in 1 M H_2SO_4 solution. As shown in Fig. S9, it can be seen that the electrode exhibits almost no loss in the current signal after 40 cycles, which suggests that catalyst of **1**-CPE has high stability.

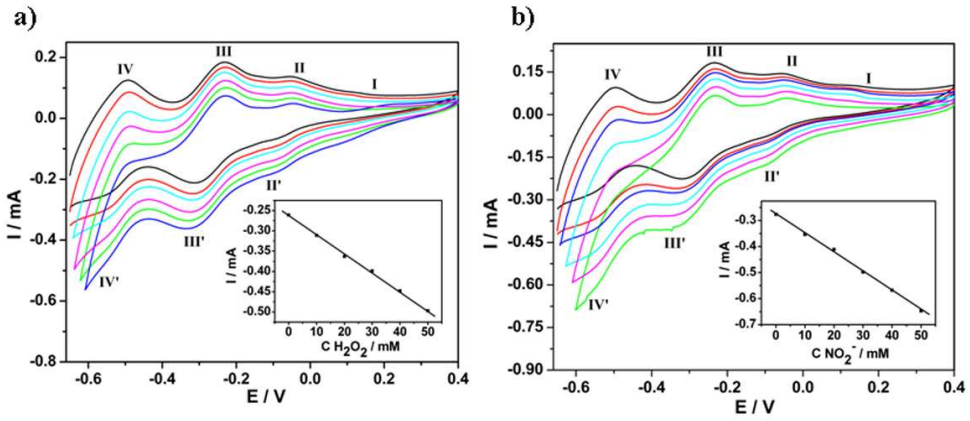

Fig. 5. Reduction of H_2O_2 (a) and NO_2^- (b) at **1**-CPE in 1 M H_2SO_4 solution containing H_2O_2 and NO_2^- in various concentrations (from inner to outer): 0, 10, 20, 30, 40, 50 mM. The inset shows a linear dependence of the cathodic catalytic current of wave IV with H_2O_2 and NO_2^- concentration, respectively.

Photocatalytic Properties

The use of POMs as photocatalysts to decompose waste organic molecules so as to purify the water resources has attracted great attention in recent years. The

introduction of transition-metal complexes as functional groups into POMs can enrich their potential applications.[39] Herein, to investigate the photocatalytic activities of compound **1** as catalysts, the photodecomposition of Methylene Blue (MB) is evaluated under UV light irradiation through a typical process: the power of 50 mg was mixed together with 100 ml of a 2.0×10^{-5} mol/L (C_0) solution of MB. Then, the mixture was continuously stirred under UV irradiation from a 250 W high-pressure Hg lamp. At 0, 30, 60, 90, 120 and 150 min, the sample (3 ml) was taken out from the beaker respectively, followed by several centrifugations to remove the new compound and a clear solution was obtained for UV-*vis* analysis.

As shown in Fig.6, after irradiation compound **1** for 150 min, the photocatalytic decomposition rate, defined as $1 - C/C_0$, is 67.8 % for **1**. In contrast, the photocatalytic decomposition rate using insoluble $(NBu_4)_6[As_2W_{18}O_{62}]$ as catalyst is 31.7 % and the blank MB solution without any catalyst is 15.9 %, which illustrates that the formation of organic-inorganic hybrid compound based on POMs could improve the photocatalytic performance of the $(NBu_4)_6[As_2W_{18}O_{62}]$. The enhanced photocatalytic property may be arisen from the following: One is the Cu-btb MOFs of **1**, which may act as photosensitizer under UV light, namely, promoting transition of electrons onto POMs; Another is the reduced-polyanion $[As_2W^{V}_2W^{VI}_{16}O_{62}]^{8-}$, which possesses the higher charge density and exert considerable influence on the pseudo-liquid phase behaviour of POMs. The photocatalytic mechanisms may be deduced as follows: during the photocatalytic reaction, $[*As_2W^{V}_2W^{VI}_{16}O_{62}]^{8-}$ (*POM) abstract electrons from water molecules and hold the electrons (Equations (1) and (2)). The reduced

POM (POM^-) is quite stable, but is rapidly re-oxidized in the presence of O_2 through Equation (3). The main function of O_2 in the POM reactions seems to be the re-oxidation (regeneration) of the catalyst. The re-oxidation step accompanies the generation of superoxides. These cycles occur continuously whilst the system is exposed to UV light. Furthermore, the MB dye is also excited by UV light to generate *MB molecules, as shown in Equation (4). Finally, after several photo-oxidation cycles, degradation of the MB dye by hydroxyl radicals and superoxides occurs (Equation (5)).[40]

$$[*As_2W^{V}_2W^{VI}_{16}O_{62}]^{8-} + h\nu \rightarrow [*As_2W^{V}_2W^{VI}_{16}O_{62}]^{8-} \quad (1)$$

$$[*As_2W^{V}_2W^{VI}_{16}O_{62}]^{8-} + H_2O \rightarrow [As_2W^{V}_2W^{VI}_{16}O_{62}]^{9-} + H^+ + OH^{\cdot} \quad (2)$$

$$[As_2W^{V}_2W^{VI}_{16}O_{62}]^{9-} + O_2 \rightarrow [*As_2W^{V}_2W^{VI}_{16}O_{62}]^{8-} + O_2^{-} \quad (3)$$

$$MB + h\nu \rightarrow *MB \quad (4)$$

$$*MB + OH^{\cdot} + O_2^{-} \rightarrow \text{intermediate products} \rightarrow \text{degradation} \quad (5)$$

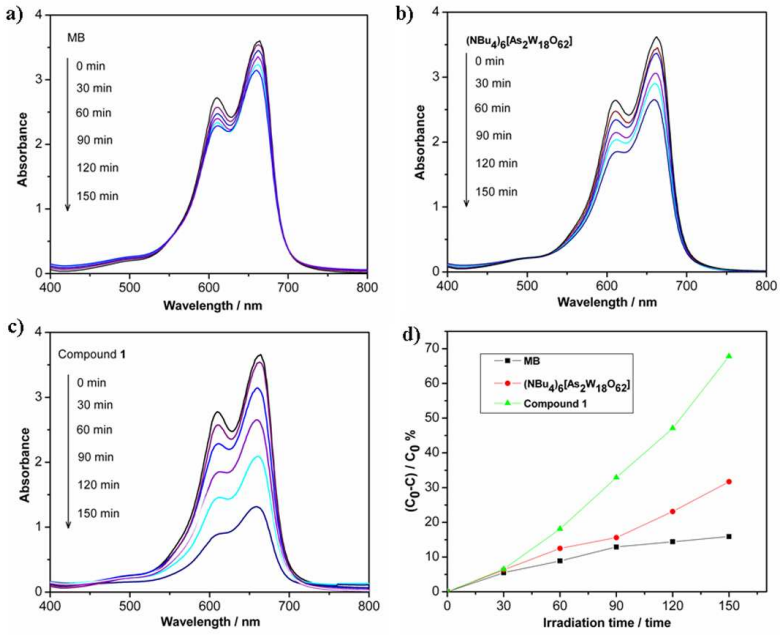

Fig. 6. Absorption spectra of the MB aqueous solution during the photodegradation under 250 W

Hg-lamp irradiation with (a) no catalyst, (b) $(NBu_4)_6[As_2W_{18}O_{62}]$ power, (c) compound **1**, and (d) conversion rate of MB with the reaction time.

Conclusion

In summary, a novel compound with 3D framework have been synthesized under hydrothermal conditions, in which reduced Wells-Dawson arsenotungstates As_2W_{18} clusters are connected to eight copper ions. The successful isolation **1** not only provides intriguing example of high dimensional and highly connected POM-based hybrid compound, but also shows that the reduced Wells-Dawson polyoxoanions, thanks to their high negative charge density, present a very useful ability to act as multi-connectors towards metal cations, opening the door to the synthesis of many more charming high-connected and high-dimensional hybrid compounds with a simple synthetic strategy. A further work in this field is underway in our laboratory.

Acknowledgments.

This work was financially supported by the NSF of China (No.21371041 and 21101045), the NSF of Heilongjiang Province (No.B201103) and innovative research team of green chemical technology in university of Heilongjiang Province, China.

References

1 M. T. Pope, *Heteropoly and Isopoly Oxometalates*, Springer, New York, 1983.

2 M. T. Pope and A. Müller, *Angew, Chem., Int. Ed.*, 1991, **30**, 34.

3 M. T. Pope and A. Müller, (Eds.), *Polyoxometalates: from Platonic Solids to Anti-Retroviral Activity*, Kluwer Academic Publishers, Dordrecht, The Netherlands, 1994.

4 M. T. Pope and A. Müller, (Eds.), *Polyoxometalate Chemistry from Topology via*

Self-Assembly to Applications, Kluwer Academic Publishers, Dordrecht, The Netherlands, 2001.

5 C. L. Hill, *Chem. Rev.*, 1998, **98**, 1.

6 T. Yamase and M. T. Pope (Eds.), *Polyoxometalate Chemistry for Nano-Composite Design*, Kluwer Academic Publishers, Dordrecht, The Netherlands, 2002.

7 J. Zhang, Y. F. Song, L. Cronin, T. B. Liu, *J. Am. Chem. Soc.*,2008, **130**, 14408.

8 D. L. Long, E. Burkholder and L. Cronin, *Chem. Soc. Rev*., 2007, **36**, 105.

9 S. T. Zheng and G. Y. Yang, *Chem. Soc. Rev.*, 2012, **41**, 7623.

10 (*a*) D. Y. Du, L. K. Yan, Z. M. Su, S. L. Li, Y. Q. Lan and E. B. Wang. *Coord. Chem. Rev*., 2013, **257**, 702; (*b*) A. Dolbecq, E. Dumas, C. R. Mayer and P. Mialane, *Chem. Rev.*, 2010, **110**, 6009.

11 (*a*) F. J. Ma, S. X. Liu, C. Y. Sun, D. D. Liang, G. J. Ren, F. Wei, Y. G. Chen, and Z. M. Su, *J. Am. Chem. Soc.*, 2011, **133**, 4178; (*b*) J. Song, Z. Luo, D. K. Britt, H. Furukawa, O. M. Yaghi, K. I. Hardcastle and C. L. Hill, *J. Am. Chem. Soc.*, 2011, **133**, 16839; (*c*) J. Zhang, J. Hao, Y. G. Wei, F. P. Xiao, P. C. Yin and L. S. Wang, *J. Am. Chem. Soc.*, 2010, **132**, 14; (*d*) G. G. Gang, F. Y. Li, L. Xu, X. Z. Liu and Y. Y. Yang, *J. Am. Chem. Soc.*, 2008, **130**, 10838.

12 (*a*) P. J. Zapf, C. J. Warren, R. C. Haushalter, and J. Zubieta, *Chem. Commun.*, 1997, 1543; (*b*) G. Férey, *Chem. Mater.* 2001, **13**, 3084; (*c*) P. Kögerler and L. Cronion, *Angew, Chem., Int. Ed.*, 2005, **44**, 844; (*d*) L. S. Long, *CrystEngComm.*, 2010, **12**, 1354.

13 (*a*) Y. Wang, Y. Peng, L. N. Xiao, Y. Y. Hu, L. M. Wang, Z. M. Gao, T. G. Wang, F. Q. Wu, X. B. Cui and J. Q. Xu, *CrystEngComm.*, 2012, **14**, 1049; (*b*) S. Aoki, T. Kurashina, Y. Kasahara, T. Nishijima and K. Nomiya, *Dalton Trans.*, 2011, **40**, 1243.

14 (*a*) C. Inman, J. M. Knaust and S. W. Keller, *Chem. Commun.*, 2002, 156; (*b*) H. Y. Liu, H. Wu, J. Yang,. Y. Y. Liu, J. F. Ma and H. Y. Bai, *Cryst. Growth Des.*, 2011, **11**, 1786; (*c*) X. F. Kuang, X. Y. Wu, J. Zhang and C. Z. Lu, *Chem. Commun*., 2011, **47**, 4150.

15 D. Hagrman, P. J. Hagrman and J. Zubieta, *Angew. Chem. Int. Ed.*, 1999, **38**, 3165.

16 L. C. W. Baker, V. S. Baker, K. Eriks, M. T. Pope, M. Shibata, O. W. Rollins, J. H. Fang and L. L. Koh, *J. Am. Chem. Soc.*, 1966, **88**, 2329.

17 (*a*) J. R. Galán-Mascarós, C. Giménez-Saiz, S. Triki, C. J. Gómez-Garcıá, E. Coronado and L. Ouahab, *Angew. Chem. Int. Ed. Engl.*, 1995, **34**, 1460; (*b*) E. Coronado, J. R. Galán-Mascarós, C. Giménez-Saiz, C. J. Gómez-García and S. Triki, *J. Am. Chem. Soc.*, 1998, **120**, 4671; (*c*) H. T. J. Evans, T. J. R. Weakley and G. B. Jameson, *J. Chem. Soc., Dalton Trans.*, 1996, 2537; (*d*) Q. Z. Zhang, and C. Z. Lu, *Z. Anorg. Allg. Chem.*, 2006, **632**, 330; (*e*) Y. Lu, Y. Xu, E. B. Wang, Y. G. Li, L. Wang, C. W. Hu and L. Xu, *J. Solid State Chem.*, 2004, **177**, 2210; (*f*) J. Y. Niu, Z. L. Wang and J. P. Wang, *J. Solid State Chem.*, 2004, **177**, 3411; (*g*) N. Honma, K. Kusakab and T. Ozeki, *Chem. Commun.*, 2002, 2896; (*h*) J. W. Zhao, Q. X. Han, P. T. Ma, L. J. Chen, J. P. Wang, J. Y. Niu, *Inorg. Chem. Commun.*, 2009, **12**, 707; (*i*) S. Lu, Y. G. Chen, D. M. Shi and H. J. Pang, *Inorg. Chim. Acta*, *2008*, **361**, 2343.

18 (a) Y. Lu, Y. Xu, E. B. Wang, J. Lü, C. W. Hu and L. Xu, *Cryst. Growth Des.*, 2005, **5**, 257; (*b*) L. S. Felices, P. Vitoria, J. M. Gutiérrez-Zorrilla, L. Lezama and S. Reinoso, *Inorg. Chem.*, 2006, **45**, 7748; (*c*) A. X. Tian, X. J. Liu, J. Ying, D. X. Zhu, X. L.Wang and J. Peng, *Inorg. Chem. Commun.*, 2011, **14**, 697.

19 (*a*) J. J. Altenau, M. T. Pope, R. A. Prados and H. So, *Inorg. Chem.*, 1975, **14**, 417; (*b*) A. Tézé, E. Cadot, V. Béreau and G. Hervé, *Inorg. Chem.*, 2001, **40**, 2000; (*c*)

H. H. Yu, X. B. Cui, J. W. Cui, L. Kong, W. J. Duan, J. Q. Xu and T. G. Wang, *Dalton Trans.*, 2008, 195; (*d*) X. L. Wang, D. Zhao, A. X. Tian and J. Ying, *Dalton Trans.*, 2014, **43**, 5211;(e) C. J. Zhang, H. J. Pang, Q. Tang, H. Y. Wang and Y. G. Chen, *Dalton Trans.*, 2010, **63**, 7993.

20 (*a*) Y. C. Wang, L. Xu, N. Jiang, L. L. Zhao, F. Y. Li and X. Z. Liu, *CrystEngComm*, 2011, **13**, 410, (*b*) Q. G. Zhai, X. Y. Wu, S. M. Chen, Z. G. Zhao and C. Z. Lu, *Inorg. Chem.*, 2007, **46**, 5046.

21 S. B. Li, W. Zhu, H. Y. Ma, H. J. Pang, H. Liu and T. T. Yu, *RSC. Advances*., 2013, **3**, 9770.

22 (*a*) R. Z. Tong, X. Y. Ren, Z. X. Li, B. Liu, H. M. Hu, G. L. Xue, F. Fu and J. W. Wang, *J. Solid State Chem.*, 2010, **183**, 2027; (*b*) F. Yao, F. X. Meng, Y. G. Chen and C. J. Zhang, *J. Coord. Chem*., 2010, **63**, 196; (*c*) X. H. Han, L. Xu, F. Y. Li and N. Jiang, *Eur. J. Inorg. Chem*., 2011, 4564; (*d*) Y. Yang, S. X. Liu, C. C. Li, S. J. Li, G. J. Ren, F. Wei and Q. Tang, *Inorg. Chem. Commun.*, 2012, **17**, 54.

23 (*a*) A. X. Tian, J. Ying, J. Peng, J. Q. Sha, Z. G. Han, J. F. Ma, Z. M. Su, N. H. Hu and H. Q. Jia, *Inorg. Chem*., 2008, **47**, 3274; (*b*) X. L. Wang, D. Zhao, A. X. Tian and J. Ying, *CrystEngComm*., 2013, **15**, 4516.

24 (*a*) L. H. Bi, E. B. Wang, J. Peng, R. D. Huang, L. Xu and C. W. Hu, *Inorg. Chem*., 2000, **39**, 671; (*b*) R. D. Claude, F. Michel, F. Raymonde, *Inorg. Chem*., 1983, **22**, 207.

25 Sheldrick, G. M. *SADABS 2.05*; University of Göttingen: Göttingen, Germany.

26 *SHELXTL 6.10*; Bruker Analytical Instrumentation: Madison, WI, 2000.

27 J. Q. Sha, J. Peng, Y. Zhang, H. J. Pang, A. X. Tian, P. P. Zhang and H. Liu, *Cryst Growth Des*., 2009, **9**, 1708.

28 (*a*) C. J. Zhang, H. J. Pang, Q. Tang, H. Y. Wang, and Y. G. Chen, *Inorg. Chem.*

Commun., 2011, **14**, 731; (*b*) C. Qin, X. L. Wang, L. Yuan, E. B. Wang, *Cryst. Growth Des*., 2008, **8**, 2093.

29 I. D. Brown and D. Altermatt, *Acta Crystallogr. Sect. B: Struct. Sci.*, 1985, **41**, 244.

30 Y. K. Lu, X. B. Cui, Y. Chen, J. N. Xu, Q. B. Zhang, Y. B. Liu, J. Q. Xu and T. G. Wang, *J. Solid State Chem.*, 2009, **182**, 2111.

31 (*a*) Y. Q. Lan, S. L. Li, X. L. Wang, K. Z. Shao, D. Y. Du, H. Y. Zang and Z. M. Su, *Inorg. Chem.*, 2008, **47**, 8179; (*b*) X. C. Huang, J. P. Zhang, Y. Y. Lin, X. L. Yu and X. M. Chen, *Chem. Commun.*, 2004, 1100.

32 (a) R. Acerete, C. F. Hammer, L. C. W. Baker, *Inorg. Chem.*, 1984, **23**, 1478; (b) R. Contant, R. Thouvenot, *Inorg. Chem. Acta.*, 1993, **212**, 41.

33 X. D. Xi, G. Wang, B.F. Liu and S.J. Dong, *Electrochim. Acta*., 1995, **40**, 1025.

34 Z. G. Han, Y. L. Zhao, J. Peng, Y. H. Feng, J. N. Yin and Q. Liu, *Electroanalysis*. 2005, **17**, 1097.

35 (*a*) A. X. Tian, J. Ying, J. Peng, J. Q. Sha, H. J. Pang, P. P. Zhang, Y. Chen, M. Zhu, Z. M. Su, *Inorg. Chem*., 2009, **48**, 100; (*b*) C. D. Zhang, S. X. Liu, C. Y. Sun, F. J. Ma and Z. M. Su, *Cryst Growth Des*., 2009, **9**, 3655.

36 X. L. Wang, Q. Gao, A. X. Tian, H. L. Hu and G. C. Liu, *J. Solid State Chem.*, 2012, **187**, 219.

37 (*a*) B. Keita, P.D. Oliveira, L. Nadjo and U. Kortz, *Chem. Eur. J.,* 2007, **13**, 5480; (*b*) C. Pichon, P. Mialane, A. Dolbecq, J. Marrot, E. RiviLre, B. Keita, L. Nadjo and F. Secheresse, *Inorg. Chem*., 2007, **46**, 5292.

38 B. Keita, A. Belhouari, L. Nadjo and R. Contant, *J. Electroanal, Chem.* 1995, **381**, 243.

39 (a) X. Wang, M. M. Zhang, X. L. Hao, Y. H. Wang, Y. Wei, F. S. Liang, L. J. Xu

and Y. G. Li. *Cryst. Growth Des*., 2013, **13**, 3454; (b) J. Q. Sha, M. T. Li, J. W. Sun, P. F. Yan, G. M. Li and L. Zhang, *Chem. Asian J.,* 2013, **8**, 2254.

40 C. H. Wu and J. M. Chern, *Ind. Eng. Chem. Res*., 2006, **45**, 6450.

A New 3D Framework Based on Reduced Wells-Dawson Arsenotungstates as Eight-connected Linkages†

Wenlong Sun, Shaobin Li, Huiyuan Ma*, Haijun Pang*, Li Zhang and Zhuanfang Zhang

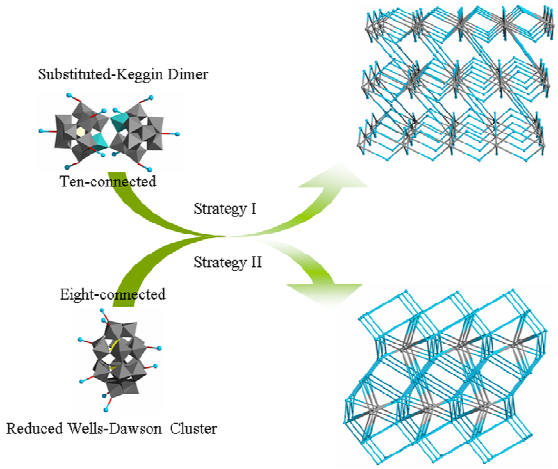

A compound representing the first example of high dimensional and high connected hybrid based on reduced Wells-Dawson arsenotungstates has been synthesized, and its electrocatalytic and photocatalytic properties have been investigated.